Phase separation and the effect of quenched disorder in $Pr_{0.5}Sr_{0.5}MnO_3$

2008 J. Phys.: Condens. Matter 20 275207

(http://iopscience.iop.org/0953-8984/20/27/275207)

J. Phys.: Condens. Matter **20** (2008) 275207 (10pp) doi:10.1088/0953-8984/20/27/275207

Phase separation and the effect of quenched disorder in $Pr_{0.5}Sr_{0.5}MnO_3$

A K Pramanik and A Banerjee

UGC-DAE Consortium for Scientific Research (CSR), University Campus, Khandwa Road, Indore-452017, MP, India

E-mail: alok@csr.ernet.in

Received 4 March 2008, in final form 30 April 2008
Published 3 June 2008
Online at stacks.iop.org/JPhysCM/20/275207

Abstract

The nature of phase separation in $Pr_{0.5}Sr_{0.5}MnO_3$ has been probed by linear, as well as nonlinear, magnetic susceptibilities and resistivity measurements across the second order paramagnetic to ferromagnetic transition (T_C) and first order ferromagnetic to antiferromagnetic transition (T_N). We found that the ferromagnetic (metallic) clusters, which form at T_C, continuously decrease their size with a decrease in temperature and coexist with non-ferromagnetic (insulating) clusters. These non-ferromagnetic clusters are identified to be antiferromagnetic. It is shown that they do not arise because of the superheating effect of the lower temperature first order transition. This reveals phase coexistence in manganite, around half-doping, encompassing two long-range order transitions. Substitution of quenched disorder (Ga) at Mn-sites promotes antiferromagnetism at the cost of ferromagnetism without adding any magnetic interaction or introducing any significant lattice distortion. Moreover, an increase in disorder decreases the ferromagnetic cluster size and with 7.5% Ga substitution cluster size reduces to the single-domain limit. Resistivity measurements also reveal the phase coexistence identified from the magnetic measurements. It is significant that, an increase in disorder up to 7.5% increases the resistivity of the low temperature antiferromagnetic phase by about four orders.

(Some figures in this article are in colour only in the electronic version)

1. Introduction

Coexistence of contrasting phases, namely, ferromagnetic (FM)–metallic (M) and antiferromagnetic (AF)–insulating (I) is a common occurrence in perovskite manganites around half-doping with generic formula $R_{0.5}A_{0.5}MnO_3$ (where R and A respectively stand for trivalent rare earth and divalent alkaline earth elements) [1]. This phase coexistence or phase separation (PS) is considered to be the factor responsible for the observed functional properties as well as the main impetus for *bi-critical* phase competition [2]. However, the origin of PS and the nature of coexisting phases remain a matter of debate [3, 4]. It is widely considered that FM–M and AF–I phases have similar energies as a result of which small perturbations, compared to thermal energy, can cause colossal changes [1, 2, 5]. This proximity in the energies of the two contrasting phases remains despite considerable changes in the nature of spin, charge and orbital ordering of the ground state with the variation in ionic radii of R/A atoms, which affects the Mn–O–Mn bonds and the one electron bandwidth (BW) [1, 2]. The decrease in average radii of R/A atoms brings about a decrease in the bandwidth and the ground state of the system changes from the so-called A-type to CE-type AF structure. This indicates that the nature of PS and the effect of quenched disorder may not remain identical as spin, charge and orbital ordering changes across the bandwidth.

It is shown that 'finite-size' clusters with large uncompensated spins are created when quenched disorder is introduced in the Mn-site of narrow BW $Pr_{0.5}Ca_{0.5}MnO_3$ having a CE-type AF and charge ordered insulating ground state [6]. Electronic phase separation gives rise to interesting effects within these clusters having some similarities with other transition metal oxides like cuprates and nickelates [7, 8]. Quenched disorder in the form of magnetic ions such as a few percent of Cr or Co in $Nd_{0.5}Ca_{0.5}MnO_3$ or $Pr_{0.5}Ca_{0.5}MnO_3$ [9, 10] and that of Fe, Cr and Ni in $La_{0.5}Ca_{0.5}MnO_3$ [11, 12] are seen to give rise to many interesting physical properties at low temperature. Interestingly, recent studies have shown that the

ground state of $Pr_{0.5}Ca_{0.5}MnO_3$ changes to FM–M even with minimal substitution of nonmagnetic disorder (2.5% Al) at Mn-sites, without introducing any significant structural distortion [4, 13]. Significantly, the conductivity of $Pr_{0.5}Ca_{0.5}MnO_3$ increases when such disorder is introduced in the Mn–O–Mn network [14]. Disorder in the form of anisotropic stress significantly changed the orbital ordering (OO) and other physical properties of $Nd_{0.5}Sr_{0.5}MnO_3$, having larger BW than $Pr_{0.5}Ca_{0.5}MnO_3$, [15]. Similarly, strain induced dimensionality crossover triggering a localization–delocalization transition is observed in $Pr_{0.5}Sr_{0.5}MnO_3$, which is an intermediate BW system with A-type AF–I ground state [16]. In the classic work of Imry and Ma [17], it was argued that random quenched disorder arising from lattice defects, dislocations or chemical substitution can destabilize the long-range order system favoring formation of 'finite-size' clusters. Appearance of coexisting clusters and their size regulation by disorder in manganites has also been shown from simulation work by Moreo *et al* [18] and Burgy *et al* has proposed chemical disorder driven inhomogeneous states across the first order transition [19]. Recently, the fragility of both the A-type and CE-type AF–I ground state against quenched disorder has been shown from computer simulation [20]. Following these experimental and theoretical developments, it becomes imperative to seriously investigate the nature of PS and the effect of disorder in different half-doped manganites.

In this context, $Pr_{0.5}Sr_{0.5}MnO_3$ (PSMO) is a very attractive system considering the A-type AF ground state where FM layers are coupled antiferromagnetically exhibiting quasi-two-dimensional (2D) metallic behavior [21, 22]. Moreover, this composition is at the phase boundary of FM and AF ground states [23], thus making it susceptible to PS, which has been observed at low temperature from the ^{55}Mn NMR study [24]. Further, PSMO has a second order paramagnetic (PM)–I to FM–M transition around 270 K and a first order FM–M to AF–I transition around 140 K [25]. Imry and Wortis [26] had predicted the rounding of the first order transition due to quenched random disorder, and beyond a certain percentage of disorder the nature of the transition is expected to change from first order to second order. Recently, it has been shown that the transformation kinetics of the first order transition in PSMO is hindered, resulting in a tunable coexisting fraction of the kinetically arrested high-T (FM) phase with equilibrium AF–I phase at low temperature [4]. Hence, substitution of quenched disorder in this system will reveal the effect on both the phase transitions as well as on the nature of PS in the same system. However, introducing quenched disorder in manganite in the form of chemical substitutions remains a challenging task, as the introduction of dissimilar ion(s) at R/A or Mn-site can lead to a change in structure, which modifies the original system completely. Apart from this, introduction of magnetic elements will also modify the basic system by introducing additional magnetic interactions.

We report here a detail study of PS in PSMO and the effect of substitutional disorder (Ga) at the Mn-site. Substitution of Ga neither adds any magnetic interaction nor introduces any significant lattice distortion since Ga^{3+} being a d^{10} element has zero orbital or spin moment and has ionic radii matching the existing Mn^{3+} [14]. An earlier study on the same substitution in PSMO has mainly focused on magneto-transport properties and shown that the high-T FM phase is suppressed and the low-T AF phase is enhanced due to the quenched disorder [27]. Thus disorder promotes AF interactions at the cost of FM in PSMO, which is contrary to the observation in $Pr_{0.5}Ca_{0.5}MnO_3$ for a similar type of substitution [13, 4]. The significant findings of the present study are summarized below. We show a drastic decrease in the FM (T_C) and an increase in the AF (T_N) transition temperatures with Ga substitution (up to 7.5%) without any significant change in structure. The change in T_C with Ga follows a simple mean-field variation indicating that no unwanted magnetic interaction is added to the system by the quenched disorder (section 3.1). The coexisting FM and non-FM clusters arise at high temperature just below T_C and persists well below T_N for all the samples. Size of the FM clusters reduces with the increase in quenched disorder (section 3.2). The FM phase fraction changes continuously as the temperature is reduced from T_C and is tracked using the second order susceptibility which directly probes the variation in the spontaneous magnetization (section 3.3). An attempt is made to identify the nature of the coexisting non-FM phase in the FM regime and it is found to be AF in nature. This observation implies that both the FM and AF phases form at T_C (section 3.4). The measured magnetic moment at 2 K agrees well with the fully spin aligned value but the moment found from fitting to the Curie–Weiss law gives a much higher value indicating the existence of FM short-range order above T_C (section 3.5). The above-mentioned nature of the coexisting phases in PSMO is substantiated through resistivity measurements which also show the drastic effect of the quenched disorder (section 3.6). The significance of this study in the context of PS and the effect of quenched disorder in the intermediate BW system around half-doping is provided in the concluding section (section 4).

2. Experimental details

Polycrystalline samples of $Pr_{0.5}Sr_{0.5}Mn_{1-x}Ga_xO_3$ series with $x = 0.0$, 0.025, 0.05 and 0.075 were prepared by the standard solid state ceramic route using Pr_6O_{11}, $SrCO_3$, MnO_2 and Ga_2O_3 with a purity more than 99.99% and the final sintering temperature used was 1500 °C for 36 h. The x-ray diffraction (XRD) measurements were made with a Rigaku Dmax 300 diffractometer with Cu Kα radiation at room temperature. All the samples were found to be in the single phase and XRD pattern were analyzed by the Rietveld profile refinement program by Young *et al* [28]. To estimate the Mn^{3+}/Mn^{4+} ratio, iodometric redox titration has been done using sodium thiosulfate ($Na_2S_2O_3{\cdot}5H_2O$) and potassium iodide (KI). The average atomic concentration in the system has been found out through an energy dispersive analysis of x-ray (EDAX) attached to transmission electron microscope (TECNAI G2-20FEI). Low field ac susceptibility measurements were performed with the home-made ac-susceptometer [29]. DC magnetization was measured with a home-made vibrating sample magnetometer (VSM) [30] and Quantum Design 14 T

Table 1. Structural parameters determined from the refinement of XRD patterns, transition temperatures and demagnetization factor (N) at temperature $\approx 0.99T_C$ for the series $Pr_{0.5}Sr_{0.5}Mn_{1-x}Ga_xO_3$. Here O1 refers to the apical oxygen of the perovskites and O2 is the equatorial oxygen which lies in the plane of the perovskite layer. The average Mn valence state of Mn was determined by iodometric titration. The extreme right column shows the percentage change ($\Delta\%$) of the parameters between the end members of the series (i.e. between $x = 0$ and 7.5%).

Ga (x)	0%	2.5%	5.0%	7.5%	$\Delta\%$
a (Å)	5.4027	5.4068	5.4044	5.4046	+0.07
c (Å)	7.7814	7.7820	7.7817	7.7791	−0.03
V (Å^3)	227.13	227.49	227.24	227.23	+0.04
Mn–O1 (Å)	1.9454	1.9455	1.9451	1.9448	−0.03
Mn–O1–Mn	180°	180°	180°	180°	0.0
Mn–O2 (Å)	1.9255	1.9274	1.9274	1.9304	+0.25
Mn–O2–Mn	165.5°	165.32°	164.89°	163.65°	−1.1
Mn^{3+}%	51.74	50.39	47.51	45.04	—
Mn^{4+}%	48.22	47.1	47.48	47.45	—
Mn valance (Av)	3.4819	3.4827	3.4994	3.5126	+0.8
T_C (K)	269.2	236.41	201.17	174.26	
T_N (K)	124.72	133.59	158.85	—	
N	0.308	0.533	0.657	—	

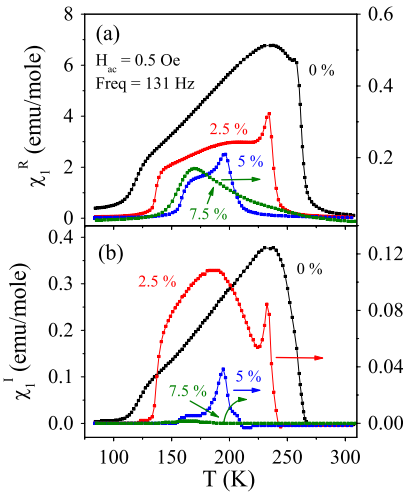

Figure 1. (a) Real and (b) imaginary parts of the first order ac susceptibility (χ_1^R and χ_1^I) measured in an 0.5 Oe ac field and 131 Hz frequency are plotted as a function of temperature for the series $Pr_{0.5}Sr_{0.5}Mn_{1-x}Ga_xO_3$.

VSM (PPMS). DC resistivity measurements were done with the standard four-probe method.

Room temperature XRD patterns were fitted and found to be in a tetragonal $I4/mcm$ space group. All the Rietveld refinement parameters and the titration results are given in table 1. The *goodness of the fit*, which is defined as the ratio of R_{wp}/R_{exp}, was found to be around 1.4 for the whole series [28]. It was found that there is no major structural distortion due to doping, as can be seen in table 1. Titration results show the average Mn valence enhances with the doping. This indicates that substituted Ga has preferentially replaced Mn^{3+} as is also expected from ionic size matching (Mn^{3+} = 0.65 Å and Ga^{3+} = 0.62 Å). The average concentration of chemical constituents found through EDAX agrees with the nominal concentration within the experimental accuracy, which is ±0.5% for the lowest Ga doped compound.

3. Results and discussions

3.1. Variation of T_C and T_N with quenched disorder

The real and imaginary part of the first order ac susceptibility (χ_1^R and χ_1^I respectively) measured for this series is shown in figures 1(a) and (b) respectively. The parent compound ($x = 0$) shows two magnetic phase transitions with decreasing temperature (PM to FM and FM to AF). For the doped samples, the PM to FM transition temperature (T_C) decreases and the FM to AF transition temperature (T_N) increases systematically. Transition temperatures are calculated from the maximum change in $d\chi/dT$ with temperature and given in table 1. For the $x = 0$ compound, T_C matches well with the reported single crystal value [25].

The large systematic change in T_C (≈100 K) without considerable structural distortion in present series is intriguing as the substituted disorder does not add any magnetic interaction to the system. We have calculated the tolerance factor (τ) for the series and found a very small change in τ (≈0.03%) between the end compositions (0% and 7.5%). To get a similar change in T_C by substitution at Ln-sites in half-doped compound $Ln_{0.5-x}Sr_{0.5}MnO_3$, a large change in τ (around 0.4–0.9%) is required [31]. Thus, the reduction of T_C in $Pr_{0.5}Sr_{0.5}Mn_{1-x}Ga_xO_3$ arises from the site dilution of the magnetic lattice and we have attempted to explain this by mean-field theory (MFT), considering only nearest neighbor interactions. According to MFT, T_C can be expressed as [32]:

$$T_C = \frac{2S(S+1)zJ}{3k_B} \tag{1}$$

where S is the average spin per magnetic ion, k_B is the Boltzmann constant, z is the number of nearest neighbor magnetic atoms and J is the exchange integral. For manganite, equation (1) has to be modified to consider possible magnetic interactions namely (i) superexchange (SE) Mn^{3+}–O^{-2}–Mn^{3+}, Mn^{4+}–O^{-2}–Mn^{4+} and (ii) double exchange (DE) Mn^{3+}–O^{-2}–Mn^{4+}. Considering these three interactions, variation of T_C with Al substitution at the Mn-sites in $LaMnO_{3+\delta}$ was explained [33]. However, for the present case we consider only an average magnetic interaction and if the Ga substitution (x) is random in the magnetic lattice, then it scales with the number of nearest neighbors (z) of equation (1). Thus a simple site dilution by Ga will result in a linear variation of T_C with x as shown in figure 2 for the experimentally found T_C. This linear scaling of T_C indicates that (i) no significant complication is introduced due to site dilution, or the average exchange integral is not modified, and (ii) substitution is random. A similar analysis for large BW manganite, $La_{0.7}Sr_{0.3}Mn_{1-x}M'_xO_3$ (M′ = Al, Ti) was used to explain the linear variation of T_C with the amount of Al as well as Ti substitutions [34]. Further, it was shown from the extrapolation of the linear variation, that T_C vanishes only when the Mn^{3+}–O^{-2}–Mn^{4+} DE interaction vanishes by the selective substitution of either Mn^{4+} or Mn^{3+} by Ti or Al

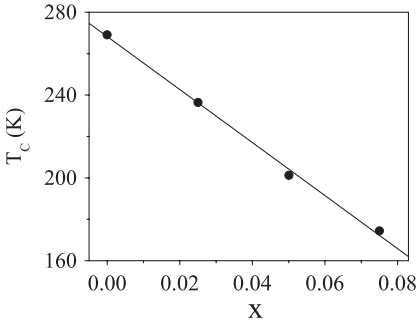

Figure 2. Variation of T_C plotted as a function of x for the $Pr_{0.5}Sr_{0.5}Mn_{1-x}Ga_xO_3$ series. This figure shows a linear decrease in T_C with an increase in disorder.

respectively. This was attributed to the dominance of the DE interaction for this large BW system. However, for the present $Pr_{0.5}Sr_{0.5}Mn_{1-x}Ga_xO_3$ series, such extrapolation (from figure 2) leads to a vanishing of T_C at $x \approx 0.21$, even when substantial amounts of both Mn^{4+} and Mn^{3+} are present. This indicates the reduction in the strength of the DE interaction with a decrease in BW.

There is a more drastic effect of quenched disorder on T_N, which appears to be counterintuitive, and certainly opposite to general antiferromagnetic systems or even the two-dimensional antiferromagnetic manganite [35]. It is clear from table 1 that T_N increases monotonically with substitution. However, the variation of T_N does not follow linear scaling with quenched disorder (x). An earlier study has shown that substitution of trivalent (In, Ga) and tetravalent (Sn, Ti) nonmagnetic elements at Mn-site in PSMO increases and decreases T_N respectively [27]. Hence, the respective change in ionic concentration and minute structural modifications arising from disorder can modify T_N in opposite ways. As seen in table 1, the Mn–O bond length in basal (O2) and apical (O1) plane has minute positive and negative changes, respectively, with disorder in this series. This can make the FM state unstable and strengthen the A-type AF state (where the FM interaction is realized along the basal plane and these planes are antiferromagnetically coupled along the apical direction) resulting in increase in T_N with disorder. However, the present experimental observations appear to contradict the theoretical proposal of the fragility of the A-type AF state against quenched disorder [20].

3.2. Phase separation and the effect of quenched disorder on it

We have probed the phase separation from the thermal hysteresis (TH) in the ac susceptibility. Figure 3(a) shows χ_1^R for the parent compound ($x = 0$) in both heating and cooling cycles. It is evident that χ_1^R shows finite TH which starts immediately below T_C and persists well below T_N. The amount of TH (χ_1^R(cooling)–χ_1^R(heating)) is given as a function of temperature in figure 3(b) for the present series. In general, TH in ac-χ has been shown to be the generic feature of a first order phase transition (FM–AF) [36]. In addition to a peak around T_N, figure 3(b) shows that the TH starts immediately below T_Cs and persists below it for all the samples. This

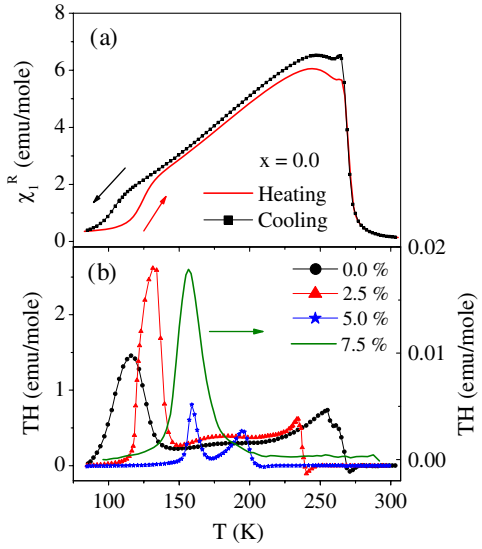

Figure 3. (a) Real part of the first order ac susceptibility (χ_1^R) measured in 0.2 Oe ac field and 131 Hz during heating and cooling for the $x = 0$ compound. (b) Temperature variation of the amount of thermal hysteresis (defined in the text) is shown for the first order susceptibility which has been measured in 9 Oe and 131 Hz for the series $Pr_{0.5}Sr_{0.5}Mn_{1-x}Ga_xO_3$.

indicates the inhomogeneous nature of the FM state where finite-size FM clusters coexist with non-FM ones. Moreover, similar TH is also observed in the variation of spontaneous magnetization measured through higher order (even order) susceptibility as well as in resistivity and will be discussed in later sections. A similar coexistence of FM and non-FM phases between T_C and T_N has also been observed for another half-doped manganite $La_{0.5}Ca_{0.5}MnO_3$ (LCMO), which has a CE-type AF ground state. Thus, phase coexistence over a large temperature window, immediately below T_C appears to be independent of the nature of spin/charge ordering and can be intrinsic to the half doped manganites. The nature of non-FM phases in LCMO has been shown to be PM around T_C and below roughly 15 K non-FM phases were found to be AF [47]. We will attempt to identify the nature of non-FM phases for PSMO in a later section.

To understand the nature of the inhomogeneous FM state we have studied the change in magnetic anisotropy as a function of both temperature and composition. The ac susceptibility shows a sharp peak in low fields immediately below T_C, as shown in figure 1(a). Enhancement of this peak height with a decrease in field can be observed for the $x = 0$ sample in figure 3(a) for 0.2 Oe compared to that shown in figure 1(a) for 0.5 Oe. Such a peak is commonly known as *Hopkinson's peak* and mainly originates due to the rapid increase in anisotropy immediately below T_C, in particular when it exceeds the applied ac field [37]. When both shape as well as magnetocrystalline anisotropies are present, the intrinsic magnetic susceptibility (χ_{int}) is related to the measured low field susceptibility (χ_{mes}) in the following way [38]:

$$\chi_{int}^{-1}(T) = \chi_{mes}^{-1}(T) - 4\pi N(T) \qquad (2)$$

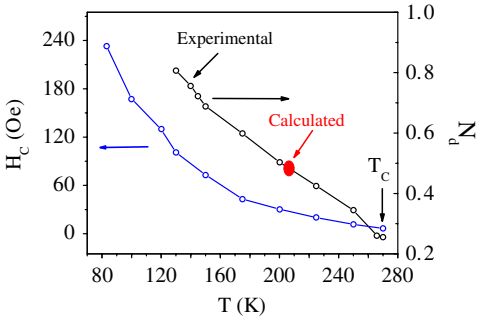

Figure 4. The left axis shows temperature variation of coercive force H_C and the right axis shows the experimentally measured demagnetization factor (N_d) in the FM regime as a function of temperature for the $x = 0$ compound. The filled symbol is the calculated N_d for the same compound.

where $N(T) = N_d + N_K(T)$, N_d is called the demagnetization factor which depends on the sample shape anisotropy and gives demagnetization field $H_d = 4\pi N_d M$ [39]. The magnetocrystalline anisotropy is taken care by N_K and for the polycrystalline FM sample, N_d is the dominant factor to anisotropy. For an FM, χ_{int} diverges at T_C in the absence of an external magnetic field and N_d depends only on the shape or dimension of the sample. Hence, the measured susceptibility in the ferromagnetic region of a homogeneous FM is expected to remain almost constant as a function of temperature (as shown in [40]). However, the significant temperature dependence in susceptibility within the FM phase (figure 1(a)) indicates a variation of magnetic anisotropy arising from the temperature dependence in N_d for the inhomogeneous FM state. Following the protocol given in [38], we have calculated N_d at different temperatures in the FM state from low field dc-magnetization data. We have also calculated the coercive field (H_C) from the hysteresis loops at various temperatures. Figure 4 shows that N_d increases with decreasing temperature for the $x = 0$ compound and exceeds the value (0.495) which was estimated from the dimension of the bulk sample [41]. This clearly indicates that N_d for an inhomogeneous FM is not given by the sample dimension but by the dimension of the 'finite-size' FM clusters within it. Moreover, variation of N_d with temperature follows the variation in the magnetic anisotropy resulting in a concomitant increase in H_C as shown in figure 4. Thus we infer from figure 4, that the FM clusters in this system spontaneously change their dimensions even well within the FM state right from their formation, and we corroborate the conclusion drawn from the observed thermal hysteresis in figure 3.

To understand the effect of quenched disorder on the inhomogeneous FM state, we have measured the variation of N_d and H_C with temperature for other samples and found qualitatively similar behavior (not shown) observed in figure 4. Table 1 shows the value of N_d at $\approx 0.99T_C$s of the respective samples, with $x = 0.0$, 0.025 and 0.05. It is clear that N_d increases with an increase in quenched disorder (x) though the bulk dimensions of all the samples are roughly same. It also implies that the increase in quenched disorder reduces the size of the FM clusters. Such a variation in 'finite-size' cluster with disorder qualitatively agrees with the earlier studies on cuprate [42].

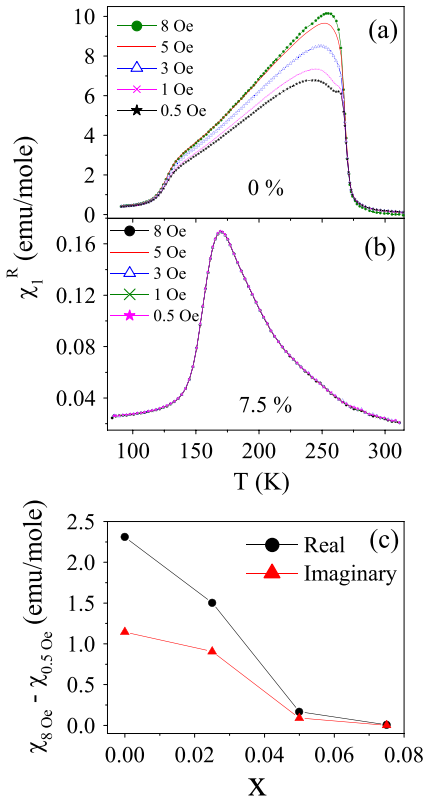

Figure 5. (a) Temperature variation of the real part of the ac susceptibility (χ_1^R) measured in different ac fields and 131 Hz frequency for the $x = 0$ compound. (b) The same field dependence has been given for $x = the0.075$ compound. (c) Difference of χ between 8 and 0.5 Oe fields as measured at $0.99T_C$ for real and imaginary parts are plotted as a function of composition (x).

We give further evidence of the decrease in FM cluster size with an increase in quenched disorder from the field dependence of ac-χ. Figure 5(a) shows χ_1^R for the parent compound in the measuring ac field range of 0.5 to 8 Oe. It is clear that the *Hopkinson's peak* immediately below T_C, though observed in 0.5 Oe, reduces and χ_1^R increases with an increase in field. As mentioned earlier, *Hopkinson's peak* which is an outcome of the rapid increase in anisotropy compared to the measurement field, is expected to decrease with an increase in field. Higher fields will help in overcoming higher pinning potentials and the domain walls will move further into the multi-domain FM clusters, giving rise to a concomitant increase in χ_1^R. On the contrary, such a field dependence is absent for the $x = 0.075$ sample (figure 5(b)) indicating that the cluster size is so small that it cannot support multiple domains. We plot the difference between the χ_1^R measured in 8 and 0.5 Oe at 0.99 T_C of the respective samples as a function of disorder (x) in figure 5(c). The observed decrease in field dependence indicates that the decrease in FM cluster size with an increase in disorder (x) actually reduces the number of domains within a cluster and approaches the single-domain limit for $x = 0.075$, where no field dependence is expected. Thus the decrease in cluster size will reduce the extent of the domain wall motion as the field is increased. Consequently, the differences between the magnetic losses for 8 and 0.5 Oe

i.e. the difference between the corresponding χ_1^I will also reduce, as shown in the figure 5(c).

3.3. Temperature variation of FM cluster size probed through second order susceptibility

The phase separated state has been probed through the variation of spontaneous magnetization as a function of both temperature as well as quenched disorder using nonlinear susceptibility (χ_2). Nonlinear susceptibilities are important experimental tools which are used to unravel intricacies about the magnetic states in different systems [6, 43, 44]. In general, magnetization (m) can be expanded in terms of magnetic field (h) as

$$m = m_0 + \chi_1 h + \chi_2 h^2 + \chi_3 h^3 + \chi_4 h^4 + \cdots \qquad (3)$$

where m_0 is the spontaneous magnetization, $\chi_1(\approx \partial m/\partial h)$ is linear and χ_2, χ_3, $\chi_4 \ldots$ are nonlinear susceptibilities. The even order susceptibilities (χ_2, $\chi_4, \ldots$) arise for the systems which have no inversion symmetry for m with respect to the applied field i.e $m(h) \neq -m(-h)$. In another way, the presence of a symmetry-breaking field is required for the experimental observation of χ_2 in ac-χ measurement. The origin of such a symmetry-breaking field can be either a superimposed external dc field or an internal field in a ferromagnet arising from spontaneous magnetization. For this reason, the second order susceptibility ($\chi_2 \approx \partial^2 m/\partial h^2$) was used to study spontaneous magnetization in different compounds [45, 46]. For a ferromagnet, as the temperature is decreased through T_C, spontaneous magnetization appears giving rise to the symmetry-breaking field, and resulting asymmetry in magnetization can be defined as $\Delta m = m(h) - (-m(-h))$. Across T_C, a sharp increase in spontaneous magnetization will result in a sharp increase in Δm. The rate of this increase will slow down as it is cooled further below T_C and may approach saturation well below T_C. Consequently, χ_2 which is proportional to $\partial \Delta m/\partial h$ will show a sharp peak around T_C, similar to the peak expected for internal $\chi_1(\approx \partial m/\partial h)$. However, this peak in χ_2 is expected to be negative since the internal field created by spontaneous magnetization is opposite to the direction of the external ac field. Moreover, χ_2 shows sharp features whenever there is sharp change in internal field and a finite value as long as there is variation in the internal field or spontaneous magnetization.

Figure 6 shows χ_2 for the series in the absence of an external dc magnetic field while heating as well as cooling the samples. While cooling from the higher temperature, χ_2 for the samples with $x = 0$, 0.025 and 0.05 appears with the onset of FM and shows a sharp negative peak around T_C. Below T_C, χ_2 shows a finite value whose magnitude decreases with temperature. On further cooling, around T_N, χ_2 again shows a comparatively small negative peak. Both the peaks around T_C and T_N indicate a sudden change in the internal field. In addition, the small peak around T_N shows considerable thermal hysteresis and shifts in peak position (insets of figure 6). This confirms a broad first order FM–AF transition in the form of supercooling and superheating of the FM/AF phases. Significantly, there is a considerable difference

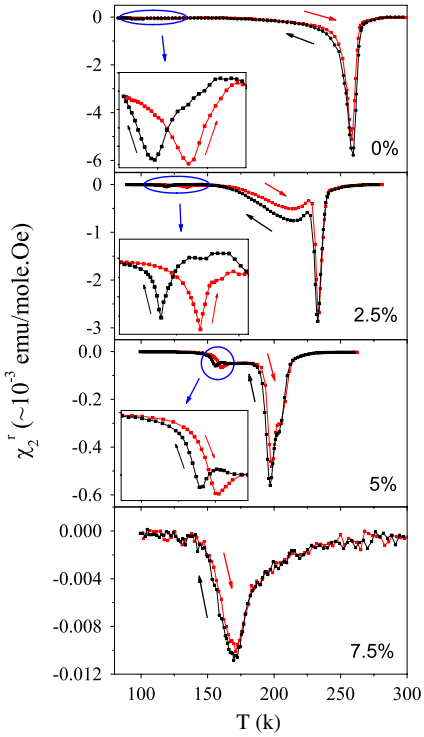

Figure 6. Temperature variation of the real part of the second order susceptibility (χ_2^R) measured during heating and cooling in an ac field of 9 Oe and frequency 131 Hz for the series $Pr_{0.5}Sr_{0.5}Mn_{1-x}Ga_xO_3$. The arrow shows the direction of the temperature cycle. Insets show the magnified view of the same plots near the broad first order FM–AF transition which clearly depict the thermal hysteresis associated with the first order transition due to supercooling and superheating of FM/AF phases.

in χ_2 between the heating and cooling runs in the FM state and around T_C. This clearly indicates a difference in the FM phase fraction in the heating and cooling run. Though such thermal hysteresis in χ_2 can be justified for a broad first order FM to AF transition, the same around the second order PM to FM transition and also within the FM state is noteworthy. Thus the coexisting phase fractions vary immediately with the onset of long-range ordering. The presence of χ_2 for the $x = 0.075$ compound in a wide temperature range shows conclusively the existence of ferromagnetism in this compound. However, this FM phase is rather inhomogeneous indicated by the broadness of the peak over a wide temperature range. This finding is quite remarkable as the susceptibility/magnetization behavior of this compound (see figure 5(b)) resembles a spin glass where χ_2 cannot exist. Moreover, magnetization of this compound looks similar to that of the $x = 0.06$ compound of the same series in [27], where it is concluded that FM vanishes with this amount of substitution. However, we show in this study that, long-range FM in PSMO exists even at a higher concentration of nonmagnetic substitution.

3.4. Phase inhomogeneity and identification of high-T non-FM phase

Now we attempt to identify the nature of the coexisting non-FM phase found immediately below T_C. The probable nature

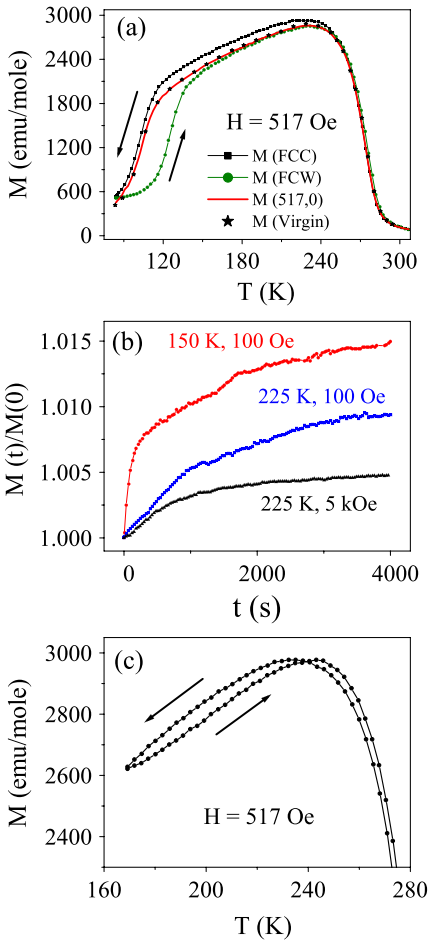

Figure 7. (a) DC Magnetization as a function of temperature measured in 517 Oe field for $x = 0$ compound. Measurements were done in FCC, FCW, $M(517, 0)$ and M(virgin) mode (defined in text). (b) Time (t) dependence of normalized magnetization has been plotted at different temperature and applied field. (c) This plot shows FCC and FCW magnetization measured in the same field but cooling was done only down to 170 K (much above T_N), showing reasonable TH in the FM state.

of it could be the high-T PM or low-T AF phase. We have measured the dc magnetization of the parent compound in 517 Oe following different protocols. Figure 7(a) shows a considerable amount of TH in FM regime between the field cooled cooling (FCC) and field cooled warming (FCW) magnetization, indicating that the coexisting phase fractions change during cooling and heating cycles. This measurement field (517 Oe) being much above the coercive field excludes the possibility that TH arise due to the effects of local anisotropy. In addition, the same measurement was repeated on the powder sample (after crushing the pellet) and we obtained a TH similar to the bulk (not shown) which rules out any possibility arising from other factors such as strain. Again, we have measured the magnetization in 517 Oe while cooling in zero field, following a rigorous protocol similar to [47]. We have started cooling the sample in zero field from above room temperature. At each measurement temperature, we isothermally apply 517 Oe field and measure the magnetization. After that, we isothermally reduce the field to zero, cool the sample to the next lower measurement temperature and repeat the above procedure for the successively lower temperatures. The magnetization measured in this protocol is shown as $M(517, 0)$ in figure 7(a). If the coexisting phase is PM (having the same structural symmetry as FM) then FM clusters will grow freely, irrespective of the way the field is applied and $M(517, 0)$ will match with the FCC data. However for a coexisting AF phase, structurally different from the FM phase, the FM clusters will not grow freely as a field is applied after cooling in zero field because of the energy barrier between the AF and FM phases. Consequently, $M(517, 0)$ will be less than the FCC data. It may be noted that in PSMO, the PM and FM phase have the same structure but there is structural change around the FM–AF transition [48]. Figure 7(a) clearly shows $M(517, 0)$ departs from FCC below T_C and gives a lower value than M(FCC) throughout the measuring temperature. This may be considered as strong evidence that the coexisting non-FM phase is AF and not PM. The present observation has some difference with the observations of [47] for another half-doped compound $La_{0.5}Ca_{0.5}MnO_3$ where $M(H, 0)$ departs from M(FCC) roughly 15 K below T_C. This has been attributed by the authors as around T_C, FM phases coexist with isostructural PM phase and below the temperature where $M(H, 0)$ and M(FCC) depart, coexisting phases are FM and AF which have different crystallographic structures. To check whether the application of a field at each measurement temperature for $M(517, 0)$ modifies the corresponding phase fraction irreversibly, we measured M(virgin) by following a different protocol. Each time we cooled the sample from the PM state to the target temperature in zero field, we isothermally applied 517 Oe to measure the magnetization M(virgin) for that temperature and repeated the complete procedure for all other temperatures. As evident in figure 7(a), there is no difference between M(virgin) and $M(517, 0)$.

The above experiment strongly suggests that the AF phase also forms around T_C and coexists with the FM phase in the ferromagnetic region. In this region, an energy barrier separates the FM and AF phase and the latter has higher energy than the former. The higher energy AF phase will be in a metastable state which has been confirmed by the time dependent magnetization. Magnetization has been measured as a function of time (t) after cooling the sample in zero field from the PM phase to the target temperature and subsequently applying a measuring field. Normalized magnetization ($M(t)/M(0)$) as a function of t is shown in figure 7(b). A continuous increase in magnetization is observed after application of 100 Oe at 225 and 150 K (within FM regime) and the same has also been observed after application of 5 kOe at 225 K. This suggests that the coexisting metastable phase (AF) tries to overcome the energy barrier to achieve the low energy FM state. The presence of the AF phase was checked by collecting FCC and FCW data at 517 Oe but cooling was done down to only 170 K which is well within the FM phase and well above T_N. Figure 7(c) shows a TH indicating the presence of the AF phase. This is a significant observation since it suggests that the presence of the AF phase at high temperature is not due to a superheating phenomenon because the sample has not approached T_N while

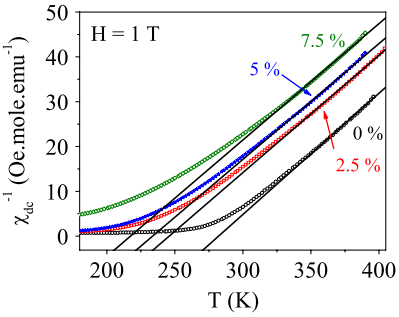

Figure 8. Inverse dc susceptibility measured in a 1 T magnetic field has been plotted as a function of temperature for the series $Pr_{0.5}Sr_{0.5}Mn_{1-x}Ga_xO_3$. Straight lines show the Curie–Weiss law fitting of susceptibility data above T_C. Data for the $x = 0.025$ compound has been shifted to higher temperature by 10 K for clarity.

Table 2. Measured μ_{eff} determined from fitting to the Curie–Weiss law, calculated μ_{eff} considering spin only value, measured and calculated saturation moment (μ) values determined from the magnetization data for the series $Pr_{0.5}Sr_{0.5}Mn_{1-x}Ga_xO_3$.

Ga (x)	0%	2.5%	5.0%	7.5%
Measured μ_{eff} (μ_B/f.u.)	5.532	5.479	5.549	5.449
Expected μ_{eff} (μ_B/f.u.)	4.396	4.286	4.161	4.038
Expected μ (μ_B/f.u.)	3.516	3.428	3.325	3.225
Measured μ (μ_B/f.u.)	3.508	3.281	3.261	3.176

cooling. Temperature variation of neutron diffraction or other microscopic experimental tools could be initiated for this compound to directly confirm the coexistence of different magnetic and structural phases as well as their variation with temperature, as has been done for $La_{0.5}Ca_{0.5}MnO_3$ in [49]. However, it may not be trivial to identify such small changes in the coexisting phase fractions unambiguously.

3.5. Evidence of short-range FM interaction above T_C

The measured magnetization in a 1 T field shows Curie–Weiss behavior, $M/H = \chi = C/(T - \theta_P)$ only from temperatures which are much higher than the respective T_Cs (figure 8). The effective Bohr magneton (μ_{eff}) per formula unit (f.u.) calculated from fitting to the Curie–Weiss law are significantly larger than the expected spin only values ($\mu_{eff} = g\sqrt{S(S+1)}$) and are given in table 2. This indicates that short-range FM interactions exist well above T_C. The existence of short-range FM interactions well above T_C was proposed for $La_{0.67}Ca_{0.33}MnO_3$ where magnetic clusters were detected from small angle neutron scattering by De Teresa *et al* [50]. This kind of magnetic clusters in the PM region have been shown for single crystal PSMO [51] and other manganites in both single crystal [52] as well as in polycrystalline samples [53] and are thought to be an intrinsic property of manganites [1]. However, the inhomogeneous phase above T_C remains a controversial issue in manganites as the short-range clusters in the PM matrix are also identified to be CE-type for different compounds [54]. It may be noted here that the field induced FM state at 2 K gives an almost fully aligned spin moment at 14 T. The measured magnetic moment (μ) per f.u. at 2 K in 14 T as well as the

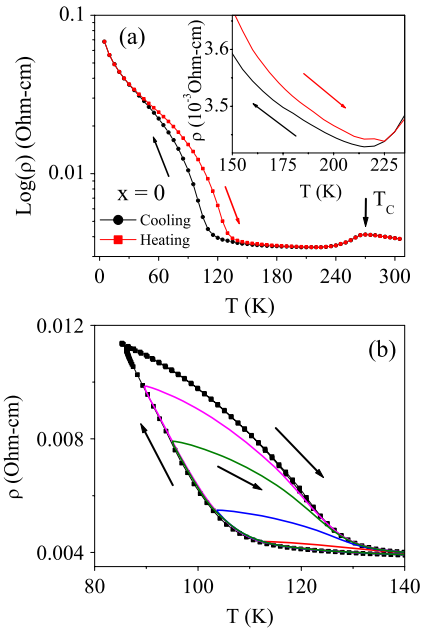

Figure 9. (a) The semi-log plot of resistivity as a function of temperature for the $x = 0$ compound measured during heating and cooling. The arrow indicates the direction of the temperature cycle. Inset shows the magnified view of thermal hysteresis in resistivity. (b) Minor hysteresis loop (MHL) around FM–AF phase transition has been plotted as a function of temperature. This plot shows a disorder broadened first order transition. The lines inside the envelope curve represent the data recorded in the heating cycle.

expected moment per f.u. calculated for the spin only value from the respective Mn^{3+} and Mn^{4+} content is given in table 2. The measured and calculated moment for the spin only value match reasonably well for all the samples.

3.6. Phase coexistence and the resistivity measurement

Resistivity measurements also substantiate the phase coexistence shown from the magnetic measurements. Figure 9(a) shows the resistivity for the $x = 0$ compound measured while heating and cooling. A metal to insulator transition (MIT) has been observed around 270 K in agreement with the single crystal measurement [25]. As the FM–AF transition is approached while cooling, the resistivity shows a steep increase accompanied by a huge thermal hysteresis, which is characteristic of a first order phase transition. Minor hysteresis loops (MHLs) are shown to be a useful method to confirm as well as study the disorder broadened first order phase transition [36, 55]. Following a similar protocol we have recorded MHLs by measuring the resistivity while cooling, to different temperatures (113, 104, 95 and 90 K) and then heating from those points all the way above T_N (figure 9(b)). MHLs are also recorded in the heating cycle (not shown) confirming a disorder broadened first order transition. It is worth noting that TH in resistivity remains well above T_N (it remains distinct up to 225 K well within the FM region) as shown in the inset of figure 9(a). It is rather significant that the resistivity being a percolative process, also confirms the change in the phase fractions well within the FM (metallic) region.

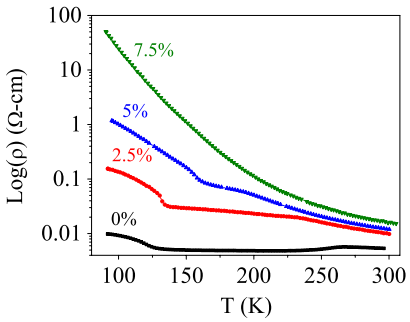

Figure 10. Resistivity data has been presented for the $Pr_{0.5}Sr_{0.5}Mn_{1-x}Ga_xO_3$ series as a function of temperature in a semi-log plot.

Figure 10 shows the resistivity for all the samples. No clear MIT was observed in the Ga substituted samples. The signature of FM–AF transition is clear from the kink in resistivity appearing around the T_N of the respective samples, with the exception of $x = 0.075$. The effect of quenched disorder is drastic and shows an increase of about 0.5×10^4 times in resistivity in the AF phase (at 92 K) with only a 7.5% substitutional disorder. Though an increase in resistivity with quenched disorder is observed in another half-doped bilayer manganite [35] the observed colossal increase in the present series is rather intriguing since, here as well, the resistivity is governed by the electrical conduction in the FM layers of the A-type AF structure. It is interesting that in an earlier study a decrease in resistivity has been observed with disorder for the CE-type AF state [14]. In view of this, and also in the context of recent theoretical developments [20], detailed investigation of the resistivity behavior of the present series needs to be undertaken.

4. Conclusion

In summary, we have studied the structural, magnetic and transport properties of half-doped $Pr_{0.5}Sr_{0.5}MnO_3$ and the effect of quenched disorder (Ga substitution) on the magnetic lattice without introducing any additional magnetic interactions or significant structural distortion. Substitution of Ga in the Mn-sites has drastic but opposite effects on the FM and AF transitions. An increase in substitutional disorder decreases T_C but increases T_N and points toward a reduction in the strength of double-exchange interaction in this intermediate BW system. The FM state is found to be inhomogeneous and the FM cluster size decreases with a decrease in temperature or an increase in quenched disorder. Significantly, the electronic phase separation gives rise to thermal hysteresis in the size of the coexisting FM and AF clusters, both of which form with the onset of long-range ordering at T_C. Moreover, the short-range FM interaction exists well above T_C. The resistivity also shows the signature of the variation of coexisting phases and substantiates the conclusion drawn from the magnetic measurements. At lower temperatures (in AF state), the resistivity shows orders of magnitude increase with quenched disorder. The observed phase coexistence needs further attention and should be probed through microscopic tools and supporting theoretical work.

Acknowledgments

We express our sincere thanks to Dr P Chaddah for many helpful discussions regarding phase coexistence. We acknowledge Dr N P Lalla for XRD and EDAX measurements. We thank Mr Kranti Kumar and Mr K Mukherjee for their help during the measurements. DST, Government of India is acknowledged for funding 14 T VSM. AKP also acknowledges CSIR, India for financial assistance.

References

[1] Dagotto E 2002 *Nanoscale Phase Separation and Colossal Magnetoresistance* (*Springer Series in Solid State Sciences* vol 136) (Berlin: Springer) and references therein
[2] Tokura Y 2006 *Rep. Prog. Phys.* **69** 797 and references therein
[3] Milward G C, Calderón M J and Littlewood P B 2005 *Nature* **433** 607
[4] Banerjee A, Pramanik A K, Kumar K and Chaddah P 2006 *J. Phys.: Condens. Matter* **18** L605
[5] Hotta T and Dagotto E 2000 *Phys. Rev.* B **61** R11879
[6] Nair S and Banerjee A 2004 *Phys. Rev. Lett.* **93** 117204
[7] Tranquada J M, Axe J D, Ichikawa N, Nakamura Y, Uchida S and Nachumi B 1996 *Phys. Rev.* B **54** 7489
[8] Tranquada J M, Nakajima K, Braden M, Pintschovius L and McQueeney R J 2002 *Phys. Rev. Lett.* **88** 075505
[9] Kimura T, Tomioka Y, Kumai R, Okimoto Y and Tokura Y 1999 *Phys. Rev. Lett.* **83** 3940
[10] Mahendiran R, Maignan A, Hébert S, Martin C, Hervieu M, Raveau R, Mitchell J F and Schiffer P 2002 *Phys. Rev. Lett.* **89** 286602
[11] Levy P, Parisi F, Granja L, Indelicato E and Polla G 2002 *Phys. Rev. Lett.* **89** 137001
[12] Martinelli A, Ferretti M, Castellano C, Cimberle M R and Ritter C 2008 *J. Phys.: Condens. Matter* **20** 145210
[13] Banerjee A, Mukherjee K, Kumar K and Chaddah P 2006 *Phys. Rev.* B **74** 224445
[14] Nair S and Banerjee A 2004 *J. Phys.: Condens. Matter* **16** 8335
[15] Wakabayashi Y, Bizen D, Nakao H, Murakami Y, Nakamura M, Ogimoto Y, Miyano K and Sawa H 2006 *Phys. Rev. Lett.* **96** 017202
[16] Uozu Y, Wakabayashi Y, Ogimoto Y, Takabo N, Tamaru H, Nagaosa N and Miyano K 2006 *Phys. Rev. Lett.* **97** 037202
[17] Imry Y and Ma S-K 1975 *Phys. Rev. Lett.* **35** 1399
[18] Moreo A, Mayr M, Feiguin A, Yunoki S and Dagotto E 2000 *Phys. Rev. Lett.* **84** 5568
[19] Burgy J, Mayr M, Martin-Mayor V, Moreo A and Dagotto E 2001 *Phys. Rev. Lett.* **87** 277202
[20] Alvarez G, Aliaga H, Sen C and Dagotto E 2006 *Phys. Rev.* B **73** 224426
[21] Kawano H, Kajimoto R, Yoshizawa H, Tomioka Y, Kuwahara H and Tokura Y 2002 *Phys. Rev. Lett.* **78** 4253
[22] Hejtmanek J, Jirak Z, Pollert E, Sedmidubsky D, Strejc A, Martin C, Maignan A and Hardy V 2002 *J. Appl. Phys.* **91** 8275
[23] Kajimoto R, Yoshizawa H, Tomioka Y and Tokura Y 2002 *Phys. Rev.* B **66** 180402
[24] Allodi G, Renzi R De, Solzi M, Kamenev K, Balakrishnan G and Pieper M W 2000 *Phys. Rev.* B **61** 5924
[25] Tomioka Y, Asamitsu A, Moritomo Y, Kuwahara H and Tokura Y 1995 *Phys. Rev. Lett.* **74** 5108
[26] Imry Y and Wortis M 1979 *Phys. Rev.* B **19** 3580

[27] Maignan A, Martin C and Raveau B 1997 *Z. Phys.* B **102** 19
[28] Young R A, Sakthivel A, Moss T S and Paiva-Santos C O 1994 *Users Guide to Program DBWS-9411* (Atlanta: Georgia Institute of Technology)
[29] Bajpai A and Banerjee A 1997 *Rev. Sci. Instrum.* **68** 4075
[30] Krishnan R V and Banerjee A 1999 *Rev. Sci. Instrum.* **70** 85
[31] Damay F, Maignan A, Martin C and Raveau B 1997 *J. Appl. Phys.* **81** 1372
[32] Kittel C 1976 *Introduction to Solid State Physics* 5th edn (New York: Wiley) chapter 15
[33] Krishnan R V and Banerjee A 2000 *J. Phys.: Condens. Matter* **12** 3835
[34] Nam D N H, Bau L V, Khiem N V, Dai N V, Hong L V, Phuc N X, Newrock R S and Nordbald P 2006 *Phys. Rev.* B **73** 184430
[35] Nair S and Banerjee A 2004 *Phys. Rev.* B **70** 104428 and references therein
[36] Manekar M, Roy S B and Chaddah P 2000 *J. Phys.: Condens. Matter* **12** L409
[37] Williams G 1991 *Magnetic Susceptibility of Superconductors and other Spin Systems* ed R A Hein, T L Francavilla and D H Liebenberg (New York: Plenum) p 482
[38] Kaul S N and Srinath S 2000 *Phys. Rev.* B **62** 1114
[39] Cullity B D 1972 *Introduction to Magnetic Materials* (Philippines: Addison-Wesley) p 49
[40] Mukherjee K and Banerjee A 2008 *Phys. Rev.* B **77** 024430
[41] Osborn J A 1945 *Phys. Rev.* **67** 351
[42] Cho J H, Chou F C and Johnston D C 1993 *Phys. Rev. Lett.* **70** 222
[43] Bajpai A and Banerjee A 1997 *Phys. Rev.* B **55** 12439
Bajpai A and Banerjee A 2000 *Phys. Rev.* B **62** 8996
Bajpai A and Banerjee A 2001 *J. Phys.: Condens. Matter* **13** 637
[44] Nair S and Banerjee A 2003 *Phys. Rev.* B **68** 094408
[45] Sinha G and Majumdar A K 1998 *J. Magn. Magn. Mater.* **185** 18
[46] Chakravarti A, Ranganathan R and Bansal C 1992 *Solid State Commun.* **82** 591
[47] Freitas R S, Ghivelder L, Levy P and Parisi F 2002 *Phys. Rev.* B **65** 104403
[48] Damay F, Martin C, Hervieu M, Maignan A, Raveau B, André G and Bourée F 1998 *J. Magn. Magn. Mater.* **184** 71
[49] Huang Q, Lynn J W, Erwin R W, Santoro A, Dender D C, Smolyaninova V N, Ghosh K and Greene R L 2000 *Phys. Rev.* B **61** 8895
[50] Teresa J M De, Ibarra M R, Algarabel P A, Ritter C, Marquina C, Balasco J, Garcia J, Moral A del and Arnold Z 1997 *Nature* **386** 256
[51] Cho S, Kang B, Zhang J and Yuan S 2006 *Appl. Phys. Lett.* **88** 172503
[52] Volkov N, Petrakovskii G, Patrin K, Sablina K, Eremin E, Vasiliev V, Molokeev M, Boni P and Clementyev E 2006 *Phys. Rev.* B **73** 104401
[53] Lu W J, Sun Y P, Song W H and Du J J 2006 *Solid State Commun.* **138** 200
[54] Kiryukhin V, Koo T Y, Borissov A, Kim Y J, Nelson C S, Hill J P, Gibbs D and Cheong S-W 2002 *Phys. Rev.* B **65** 094421 and references therein
[55] Singh K J, Chaudhary S, Chattopadhyay M K, Manekar M A, Roy S B and Chaddah P 2002 *Phys. Rev.* B **65** 094419